2.2 Confinement - Deconfinement Phasetransition

Use of propagators for computing order parameter of confinement

Preparation:

Polyakov Loop: $\beta = 1/T$

$$L(\vec{x}) = \frac{1}{N_c} \operatorname{tr} \mathcal{P} e^{ig\int_0^\beta dx_0 A_0}$$

example:

$U(1)$: $e^{ig\int_0^\beta dx_0 A_0(x)} = e^{i\int_0^\beta d^4y \, A_0(y)\, j_0(y)}$

$$j_0(y) = \int_0^\beta d\tau \, \delta^{(4)}(y - x(\tau)) \qquad , \; x_0(\tau) = \tau, \quad \vec{x}(\tau) = \vec{x}$$

worldline of static charge

Quark - antiquark potential:

$$\langle q(x)\, \bar{q}(y) \rangle = \langle L(\vec{x})\, L^{+}(\vec{y}) \rangle = e^{-F_{q\bar{q}}(|\vec{x}-\vec{y}|)}$$

Confinement: $\lim_{|\vec{x}-\vec{y}| \to \infty} \langle q(x)\, \bar{q}(y) \rangle \to 0$

$$F_{q\bar{q}} \to \infty$$

Deconfinement: $\lim_{|\vec{x}-\vec{y}| \to \infty} \langle q(x)\, \bar{q}(y) \rangle \neq 0$

$F_{q\bar{q}}$ finite

$$(\not{D} + m_q)\,\psi = 0$$

$m_q \to \infty$: $\partial_{x_i} \psi \simeq 0$ static limit (quenched)

$$\Rightarrow \quad (\not{D} + m_q)\,\psi \xrightarrow{m_q \to \infty} (D_0 \gamma_0 + m_q)\,\psi = 0$$

free quark : $(\partial_0 \gamma_0 + m_q)\,\psi_0 = 0$

Full solution:

$$\psi(x) = L(x)\,\psi_0$$

$$(D_0 \gamma_0 + m_q)\,\psi = \gamma_0 \partial_0 L(x)\,\psi_0 + i g A_0 \gamma_0 \psi$$

$$\Rightarrow \quad \partial_0 L(x) = i g A_0 L(x)$$

$$\Rightarrow L(x) = \frac{1}{N_c}\,\mathrm{tr}\,\mathcal{P}\, e^{ig\int_0^t A_0\, d\tau}$$

path ordering

Declustering:

$$\lim_{|\vec{x}-\vec{y}|\to\infty}\left(\langle q(x)\,\bar{q}(y)\rangle - \langle q(\vec{x})\rangle\langle \bar{q}(\vec{y})\rangle\right) = 0$$

(or $\langle q(x)\rangle = e^{-F_q}$

confinement: $F_q = \infty$

Deconfinement: F_q finite)

Effective action approach:

- compute $\Gamma_k[A_0^c] = V_k[A_0^c]$
- $\langle A_0\rangle = \bar{A}_0$ with $\left.\frac{\partial V_k}{\partial A_0^c}\right|_{\bar{A}_0} = 0$
- $\langle L(x)\rangle \leq 1/N_c \operatorname{tr} P e^{i\int_0^\beta \langle A_0\rangle}$

Flow of one field mode:

$$\frac{1}{2}\, T\sum_{n\in\mathbb{Z}}\int \frac{d^3q}{(2\pi)^3} \operatorname{tr}_{\mathrm{ad}} \frac{1}{\Gamma_k^{(2)}[A_0](q) + R_k(\vec{q}^{\,2})}\,\dot{R}_k(\vec{q}^{\,2})$$

with $q = (2\pi n T, \vec{q})$

$$\dot{V}_k[A_0] = \frac{1}{2}\,\mathrm{Tr}\,\frac{1}{\Gamma^{(2)}_A[A]+R_A}\,\dot{R}_A$$

$$-\,\mathrm{Tr}\,\frac{1}{\Gamma^{(2)}_c[A]+R_c}\,\dot{R}_c$$

$$= \frac{1}{2}\,T\sum_n\int\frac{d^3q}{(2\pi)^3}\,\mathrm{tr}_{ad}\,\frac{1}{Z_L(D)(-D^2)+R_L}\,\dot{R}_L$$

$$+\,2\cdot\frac{1}{2}\,T\sum_n\int\frac{d^3q}{(2\pi)^3}\,\mathrm{tr}_{ad}\,\frac{1}{Z_T(D)(-D^2)+R_T}\,\dot{R}_T$$

$$+\,\frac{1}{2}\,T\sum_n\int\frac{d^3q}{(2\pi)^3}\,\mathrm{tr}_{ad}\,\frac{1}{Z_{gauge}(D)(-D^2)+R_{gauge}}\,\dot{R}_{gauge}$$

$$-\,T\sum_n\int\frac{d^3q}{(2\pi)^3}\,\mathrm{tr}_{ad}\,\frac{1}{Z_c(D)(-D^2)+R_c}\,\dot{R}_c$$

$\mathrm{tr}_{ad}\, f(-D_0^2)$

$$p_0 = 2\pi n T$$

$$= \mathrm{tr}_{ad} f\left((2\pi n T + g A_0)^2 \right)$$

$$= \mathrm{tr}_{ad}\, f\left((2\pi T)^2 \left(n + \frac{g A_0}{2\pi T}\right)^2 \right)$$

Expand in Eigenfunctions of $g A_0$:

A_0 const. and in Cartan sub-algebra

$t^3_{fund} = \sigma^3/2 = \begin{pmatrix} 1/2 & 0 \\ 0 & -1/2 \end{pmatrix}$

$SU(2)$: $\quad A_0 = A_0^c\, t^3 \qquad t^3_{ad} = \begin{pmatrix} \sigma^3 & 0 \\ 0 & 0 \end{pmatrix} = \begin{pmatrix} 1 & \\ & 0 \end{pmatrix}$

$SU(3)$: $\quad A_0 = A_0^3\, t^3 + A_0^8\, t^8$

$$\varphi_3 = \beta g \frac{A_0^3}{2\pi}, \quad \varphi_8 = \beta g \frac{A_0^2}{2\pi}$$

$$\Rightarrow \mathrm{tr}_{ad} f\left((2\pi n T + g A_0)^2 \right)$$

$SU(2)$ $\quad = f\left((2\pi T)^2 (n+\varphi)^2 \right) + f\left((2\pi T)^2 (n-\varphi)^2 \right) + f\left((2\pi T)^2 n^2 \right)$

with $\varphi = \beta g\, A_0^c / 2\pi$

$SU(3)$ $\quad = \sum_{m=1}^{N_c^2-1} f\left((2\pi T)^2 (n + \varphi_m)^2 \right)$

$$\varphi_m = \left(\pm \varphi_3, \pm\left(\varphi_3/2 + \frac{\sqrt{3}}{2}\varphi_8\right), \pm\left(\varphi_3/2 - \frac{\sqrt{3}}{2}\varphi_8\right), 0, 0 \right)$$

$$\begin{pmatrix} 0 & -\phi 3 & 0 & 0 & 0 & 0 & 0 & 0 \\ \phi 3 & 0 & 0 & 0 & 0 & 0 & 0 & 0 \\ 0 & 0 & 0 & 0 & 0 & 0 & 0 & 0 \\ 0 & 0 & 0 & 0 & -\frac{\phi 3}{2}-\frac{\sqrt{3}\,\phi 8}{2} & 0 & 0 & 0 \\ 0 & 0 & 0 & \frac{\phi 3}{2}+\frac{\sqrt{3}\,\phi 8}{2} & 0 & 0 & 0 & 0 \\ 0 & 0 & 0 & 0 & 0 & 0 & \frac{\phi 3}{2}-\frac{\sqrt{3}\,\phi 8}{2} & 0 \\ 0 & 0 & 0 & 0 & 0 & -\frac{\phi 3}{2}+\frac{\sqrt{3}\,\phi 8}{2} & 0 & 0 \\ 0 & 0 & 0 & 0 & 0 & 0 & 0 & 0 \end{pmatrix}$$

$$\Rightarrow \mathring{V}_{SU(2)} \cong \mathring{V}_{mode}(\varphi) + \mathring{V}_{mode}(-\varphi)$$

$$\mathring{V}_{mode}(\varphi) = +\mathring{V}_{mode}(-\varphi) \quad \to \quad = 2\,\mathring{V}_{mode}(\varphi)$$

$$\mathring{V}_{SU(N)} = \sum_{m=1}^{N_c^2-1} \mathring{V}_{mode}(\varphi_m) = \frac{1}{2} \sum_{m} \mathring{V}_{SU(2)}(\varphi)$$

left out

$\boxed{SU(2):}$

Perturbation theory:

$$\mathring{V}_{pert}[A_0] = 1/2 \; T \sum_n \int \frac{d^3 q}{(2\pi)^3} \, \mathrm{tr} \frac{1}{\vec{q}^{\,2} + (2\pi n + gA_0)^2 + R(\vec{q}^{\,2})} \mathring{R}(\vec{q}^{\,2})$$

$$\left(\frac{d-1}{2} - 1/2 \right)$$

$(d-1)$ transversal

gauge mode − ghost
$1/2 - 1$

$d = 4$

$$V_{pert}[A_0] = \left[\frac{1}{\beta^4} \left[\phi^2/12 - \frac{\phi^3}{12\pi} + \frac{\phi^4}{48\pi^2} \right] \right]$$

with $\phi = g A_0$ mod 2π

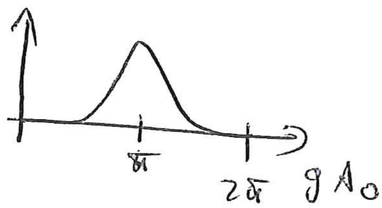

$$\Rightarrow \boxed{\bar{A}_0 = 0 \; : L(x)|_{\bar{A}_0} = 1}$$

IR: $\Gamma^{(2)}_{A/c} \simeq [-D(A_0)]^{1+k_{A/c}}$

$$\Rightarrow \mathring{V}_{IR}[A_0] = \left[\frac{d-1}{2}(1+k_A) + \frac{1}{2} - (1+k_c) \right] \mathring{V}_{pert}[A_0]$$

$$\Rightarrow V_{IR}[A_0] = \underbrace{\left[\frac{d-1}{2}(1+k_A) + \frac{1}{2} - (1+k_c) \right]}_{c(k_A, k_c)} V_{pert}[A_0]$$

(1) confinement: $c(k_A, k_c) < 0$: $\boxed{d - 2 + (d-1)k_A - 2k_c < 0}$

(2) deconfinement: $c(k_A, k_c) > 0$

Weiss potential : $V_{1\text{-loop}}$

Gross, Pisarski, Yaffe '81
Weiss '81

$$V_{\text{mode}}\Big|_{1\text{-loop}} = \frac{1}{2}\int_\infty^0 \frac{dk}{k}\, T\sum_n \int \frac{d^3p}{(2\pi)^3}\, \frac{\dot{R}_k\big((2\pi T)^2(n+\varphi)^2+\vec{p}^{\,2}\big)}{(2\pi T)^2(n+\varphi)^2+\vec{p}^{\,2}+R_k}$$

$$= \frac{1}{2}\int_\infty^0 \frac{dk}{k}\, T\sum_n \int \frac{d^3p}{(2\pi)^3}\, \partial_t \ln\Big[(2\pi T)^2(n+\varphi)^2+\vec{p}^{\,2}+R_k\Big]$$

$$\simeq \frac{1}{2}\, T\sum_n \int \frac{d^3p}{(2\pi)^3}\, \ln\Big[(2\pi T)^2(n+\varphi)^2+\vec{p}^{\,2}\Big]$$

[Normalisation : $V_{\text{mode}}(\varphi) \Rightarrow V_{\text{mode}}(\varphi) - V_{\text{mode}}(0)$]

$$\frac{1}{2}\, T\sum_n \int \frac{d^3p}{(2\pi)^3}\Big\{\ln\Big[(2\pi T)^2(n+\varphi)^2+\vec{p}^{\,2}\Big] - \ln\Big[(2\pi T)^2 n^2+\vec{p}^{\,2}\Big]\Big\}$$

contour-int. of $\partial_{\vec{p}^2}\sum_n\{\ \}$

$$= \frac{1}{2}\, T\int \frac{d^3p}{(2\pi)^3}\Big\{\ln\Big[\cosh\beta|\vec{p}| - \cos 2\pi\varphi\Big] - \ln\Big[\cosh\beta|\vec{p}| - 1\Big]\Big\}$$

$$\simeq \frac{1}{2}\, T\int \frac{d^3p}{(2\pi)^3}\, \ln\Big[1 - 2e^{-\beta|\vec{p}|}\cos 2\pi\varphi + e^{-2\beta|\vec{p}|}\Big]$$

Now we use

$$\ln\left[1-2\,e^{-\beta|\vec p|}\cos 2\pi\varphi + e^{-2\beta|\vec p|}\right]$$

$$= \mathrm{Re}\,\ln\left(1-e^{-\beta|\vec p|}\,e^{2\pi i\varphi}\right)$$

$$= \mathrm{Re}\sum_{n=1}^{\infty}\frac{1}{n}e^{-\beta|\vec p|n}\,e^{2\pi i n\varphi}$$

to wit

$$V_{\text{mode}}(\varphi)\simeq T\int_0^\infty \frac{dp}{(2\pi)^2}\,p^2\,\ln\left[\qquad\right]$$

$$\simeq \frac{1}{4\pi^2}T^4\sum_{n=1}^{\infty}\int_0^\infty d\hat p\,\hat p^2\,\frac{1}{n^4}e^{-\hat p}\,e^{2\pi i n\varphi}$$

$$\hat p = \beta n|\vec p|$$

$$\simeq \frac{1}{4\pi^2}T^4\sum_{n=1}^{\infty}\frac{1}{n^4}\,e^{2\pi i n\varphi}$$

$$\boxed{\Rightarrow \beta^4 V_{\text{mode}}(\varphi) = -\frac{2}{3}\pi^2\left(\tilde\varphi-\tfrac12\right)^2+\frac{4}{3}\pi^2\left(\tilde\varphi-\tfrac12\right)^4+\frac{\pi^2}{12} = \frac{\pi^2}{12}\left[4\left(\tilde\varphi-\tfrac12\right)^2-1\right]^2}$$

$$\tilde\varphi = \varphi \bmod 2\pi$$

Ph D - Markus Q. Huber

Results for $SU(2)$

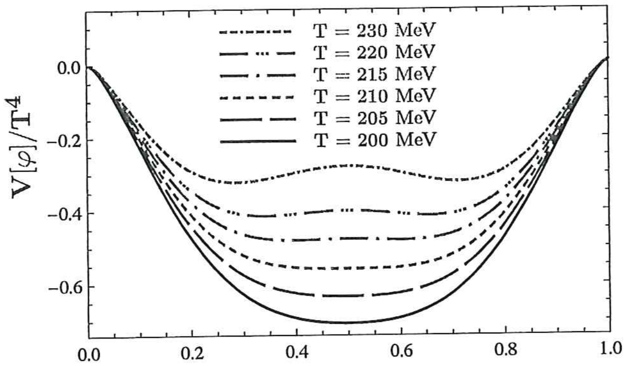

(a) Polyakov loop potential for $SU(2)$. For low temperatures the minimum is at the confining value $\varphi = 1/2$ for $SU(2)$. For higher temperatures the minimum moves to a different value which signals the deconfinement-confinement phase transition.

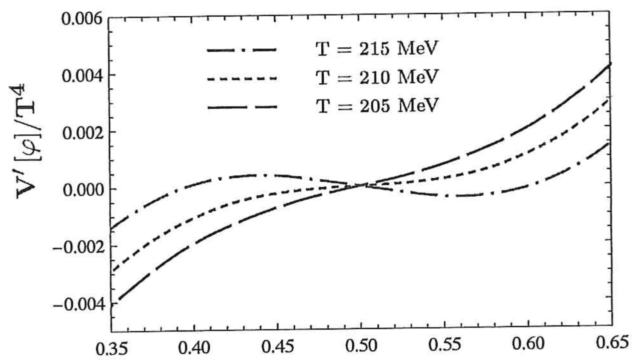

(b) At the phase transition temperature the derivative of the Polyakov potential for $SU(2)$ changes at the confining value from a positive to negative slope, turning the minimum of the potential into a local maximum.

Figure 5.7.: Polyakov loop potential for $SU(2)$ from its DSE representation with vacuum scaling propagators.

Eq. (5.33) only depends on the ghost and gluon propagators. In the following three different kinds of propagators are used. At first, the difference between the decoupling and the scaling solutions of Yang–Mills propagators at vanishing temperature, cf. section 2.3.2, is studied.
Similar to the pressure, cf. section 4.3, the finiteness of the temperature has a two-fold effect. On the one hand side, the Matsubara sum yields an explicit dependence and on the other hand side, the wave-function renormalisation are temperature dependent. Therefore, the third approximation for the Polyakov loop potential is obtained with the temperature-dependent propagators presented in chapter 4.

The Polyakov loop potential for $SU(2)$ from the scaling propagators at vanishing temperature is given in fig. (5.7(a)). As argued before the position of the minimum decides about a confining ($\varphi = 1/2$) or deconfining ($\varphi \neq 1/2$) potential. In fig. (5.7(a)) the Polyakov loop potential is given at different temperatures, the critical temperature T_c for the deconfinement-confinement phase transition is obtained best by the help of the derivative of the Polyakov loop potential, which is plotted in fig. (5.7(b)). The phase transition happens at the point at which the minimum in the potential moves away from $\varphi = 1/2$. As it is a smooth transition, the potential is flat around $\varphi = 1/2$ at this temperature. Thus, a vanishing derivative of the potential in this region signals the phase transition. Being computed from the scaling propagators the critical temperature is $T_c^{\text{scal}} \approx 210\,\text{MeV}$. In comparison to this, the FRG result gives a critical temperature of $T_c^{\text{FRG}} \approx 266\,\text{MeV}$ in [11], using the same input. However, note that the two-loop diagram has been omitted in the computation presented here which could potentially correct for this deviation.

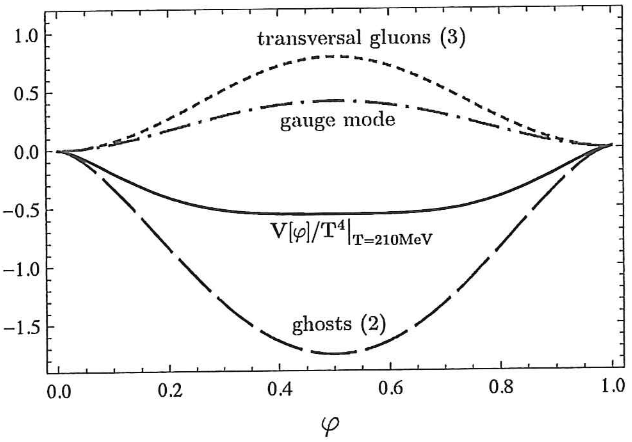

Figure 5.8.: Individual contributions from the gauge mode, the transversal gluons and the ghost loop with trivial implicit temperature dependence in the Polyakov loop potential obtained from its presentation in the framework DSEs.

Functional methods have the advantage that often the mechanisms and individual contributions can be resolved. In this case it is trivially possible due to the additive structure of the equation for the potential, eq. (5.33). As outlined above the gauge mode gives half of the perturbative one-loop potential. The factor of one-half stems from the fact that the perturbative potential is made up from the two physical modes: the transverse polarisations of the gluon. The Polyakov loop potential is gauge invariant, thus only the physical modes must contribute. Naturally, the perturbative result simply reproduces this feature. In fact, for trivial propagators all different modes contribute combinatorically with the same weight. So the cancellation of the unphysical modes can be understood easily. All of the four gluonic degrees of freedom contribute equally with $\frac{1}{2}V^{\text{Weiss}}_{SU(N_c)}$ each. The amplitude of the ghost potential is equal to this, however, these modes contribute with a negative sign. So a trivial summation cancels the two unphysical mode, leaving exactly $V^{\text{Weiss}}_{SU(N_c)}$.

PhD-Thesis L. Fister

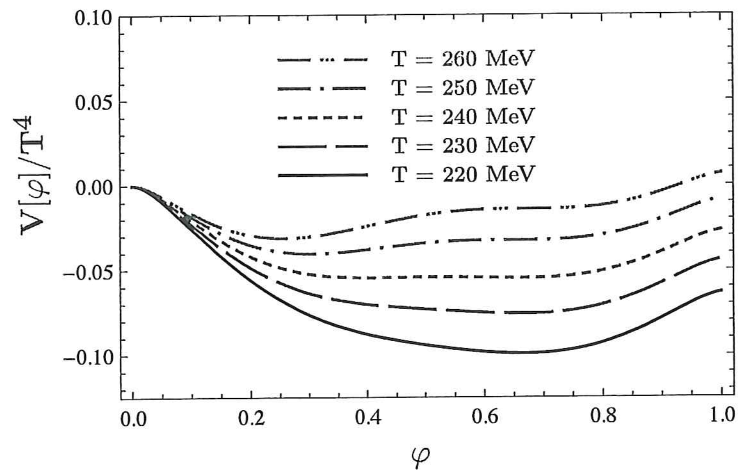

(a) Polyakov loop potential for $SU(3)$ obtained from temperature-independent scaling propagators from [276].

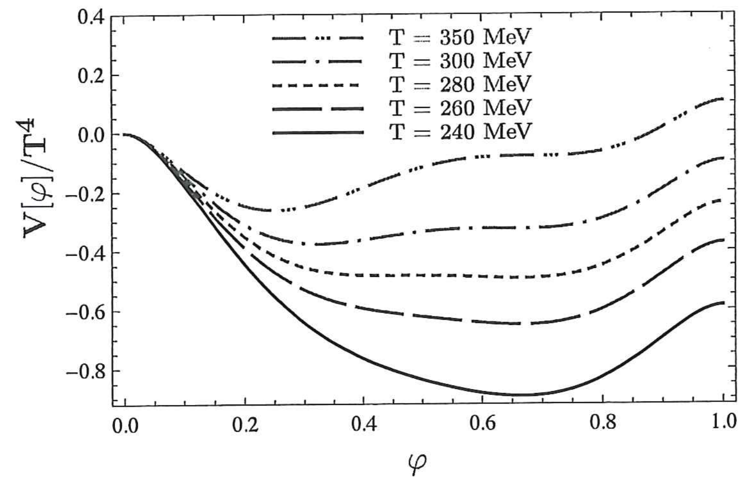

(b) Polyakov loop potential for $SU(3)$ obtained from temperature-dependent propagators from chapter 4.

Figure 5.13.: The Polyakov loop potential for $SU(3)$ can be obtained from the $SU(2)$ potential according to eq. (5.37). This figure shows the $SU(3)$ potential in the $\varphi = \varphi^3$ direction. The confining value is $\varphi = 2/3$. The position of the minimum serves as an order parameter for the deconfinement-confinement phase transition. At the critical temperature it jumps from its confining value to a non-confining value. This signals a first order phase transition for $SU(3)$, which is in agreement with lattice results, see e.g. [20].

tures for the deconfinement-confinement phase transition in $SU(2)$ and $SU(3)$ obtained from the best truncation within functional methods agree well with lattice gauge theory, there are caveats arising from truncations. Thus, the high accuracy may be a lucky coincidence. Nevertheless, it is fair to infer from the previous results that the occurence of the phase transition at the correct order of magnitude is definitely not affected by these approximations. In the following I summarise the potential problems and arguments why

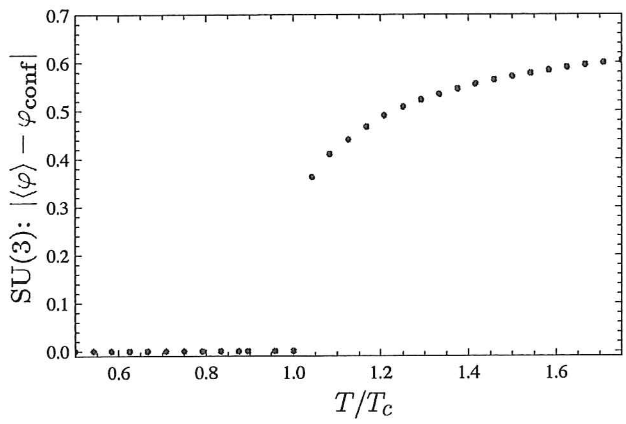

Figure 5.14.: First order phase transition for $SU(3)$ obtained from temperature-independent scaling propagators. The expectation value of the temporal gluon serves as an order parameter for the deconfinement-confinement phase-transition. The confining value for $SU(3)$ is $\varphi_{\mathbf{conf}} = 2/3$.

these deviations from the lattice in the corresponding parts could be subleading in the computation of the Polyakov loop potential.

Firstly, the main ingredients for the DSE representation of the Polyakov loop potential are the propagators. The good agreement is achieved with the temperature-dependent propagators given in chapter 4. For the temperatures of the phase transitions the results for the chromomagnetic gluon and the ghost are in satisfactory agreement with the lattice. In contrast to this, the chromoelectric propagator is significantly enhanced on the lattice. This is not seen in the FRG. However, the FRG propagator is evaluated on a non-trivial background. The background is identified with the Polyakov loop potential which is directly sensitive to the critical physics, in contradistinction to the computations of the thermal propagators presented in section 4.2.1. Therefore, although there is a clear deviation in the propagators, the way in which they occur in the subsequent computations may correct for this. This conjecture is supported by the quantitative agreement of the pressure given in fig. (4.3).

Secondly, another benchmark for the DSE Polyakov loop potential are the FRG results, which give higher critical temperatures for the same input. Since in the one-loop truncation of the DSE only the propagators enter, this may be due to the missing two-loop contribution. However, the two-loop contribution can be approximated by a diagram which has the same structure as the one-loop gluon term but with a three-gluon vertex correction. This vertex correction is supposedly a small correction. The latter statement is based on the results for the two-point functions at vanishing temperature in the DSE framework [276] given in section 2.3.2 in fig. (2.4), in which the two-loop diagrams have been dropped. Nevertheless, these results show that the main contributions arise from the one-loop diagrams and the two-loop terms give a small correction. This suggests that the two-loop diagram in the DSE representation of the Polyakov loop potential gives only a small correction as well.

Determination of $\Gamma_k^{(2)}[A_0]$:

(a) $\Gamma_k^{(2)}[A_0] = \Gamma^{(2)}_{k,\,\text{Landau}}\left(-D^2(A_0)\right) + A_0\text{-terms}$

$$\Gamma_k^{(2)}[A_0]\Big|_{A_0=0} = \Gamma^{(2)}_{k,\,\text{Landau}}(p^2)$$

Can we do better? $\Rightarrow$ Background field gauge

Landau gauge $\longrightarrow$ Landau-DeWitt gauge

gauge: $\partial_\mu A_\mu = 0 \longrightarrow D_\mu(\bar{A})\, a_\mu = 0$

FP: $-\partial_\mu D_\mu(A) \longrightarrow -D_\mu(\bar{A}) D_\mu(A)$

with $A_\mu = \bar{A}_\mu + a_\mu$; fluctuation field, background field

. 'gauge invariant' gauge condition

background gauge trafos $\bar{\delta}$: $a_\mu \xrightarrow{1+\bar{\delta}} a_\mu - [a_\mu, \omega]$, $\bar{A}_\mu \xrightarrow{1+\bar{\delta}} \bar{A}_\mu - [D_\mu(\bar{A}), \omega]$ $\Big\}$ $A_\mu \xrightarrow{1+\bar{\delta}} A_\mu - [D_\mu(A), \omega]$

fluct. field trafo : $a_\mu \xrightarrow{1+\delta} a_\mu - [D_\mu, \omega]$, $\bar{A}_\mu \xrightarrow{1+\delta} \bar{A}_\mu$ $\Big\}$ $A_\mu \xrightarrow{1+\delta} A_\mu - [D_\mu(A), \omega]$

Gauge-inv.: $\delta(c,\bar{c}) = \bar{\delta}(c,\bar{c}) = -[\omega, (c,\bar{c})]$, $\phi = (a, c, \bar{c})$

$\bar{\delta}\, D(\bar{A}) a_\mu = -[\omega, D_\mu(\bar{A}) a_\mu]$

$\bar{\delta}(-D_\mu(\bar{A}) D_\mu) = -[\omega, -D_\mu(\bar{A}) D_\mu)]$ $\Big\}$ $\boxed{\bar{\delta}\, S[\phi, \bar{A}] = 0}$

$$\Rightarrow \quad \bar{\delta}\, \Gamma_k[\phi, \bar{A}] = 0$$

e.g.: $\int d^dx \; a_\mu^a \, R^{ab}_{k\,\mu\nu}(-D^2(\bar{A}))\, a_\nu^b + \ldots$

with $\boxed{\bar{\delta}\, R_k = -[\omega, R_k]}$

$$\Rightarrow \bar{\delta} \frac{\delta^2}{\delta a^2} \Gamma_k \Big|_{a=0} = -\Big[\omega, \frac{\delta^2 \Gamma_k}{\delta a^2}\Big|_{a=0}\Big]$$

$A = \bar{A}$

$$\Rightarrow \quad \frac{\delta^2 \Gamma_k}{\delta a^2}\Big|_{a=0} = \Gamma^{(2)}_{k,\,\text{Landau}}(-D^2(A)) + F_{\mu\nu}\text{-terms}$$

$$F_{\mu\nu}(A = A_0) = 0$$

[finite T: + $L(\vec{x})$-dep. terms]

$\Rightarrow$ $\boxed{\text{Slides}}$

$$\boxed{V^{IR} = \left(\frac{1 + (d-1)\kappa_A - 2\kappa_c}{d-2}\right) V^{UV}}$$

Criterion:

$$\boxed{(d-1) + (d-1)\kappa_A - 2\kappa_c < 0}$$

$\kappa_A = -2\kappa_c - \frac{4-d}{2}$: $\boxed{\kappa_c > \frac{d-3}{4}}$

4d:

$$\boxed{\begin{array}{l} 2 + 3\kappa_A - 2\kappa_c < 0 \\ \kappa_A = -2\kappa_c : \quad \kappa_c > 1/4 \end{array}}$$

FRG / DSE: $\kappa_c \simeq \frac{93 - \sqrt{1201}}{98} = 0.595353\ldots$

$$2 + 3\kappa_A - 2\kappa_c \simeq -6.76 < 0$$

Lattice: $\kappa_A \simeq -1$, $\kappa_c \simeq 0$

$$\Rightarrow 2 + 3\kappa_A - 2\kappa_c \simeq -1 < 0$$

Numerics:

num. accuracy

$SU(2)$: $T_c \simeq 276 \pm 10\,\text{MeV}$ $\qquad T_c/\sqrt{\sigma} = 0.614 \pm 0.023$

est. syst. error: $\approx 20\%$ $\qquad$ lattice: 0.709

est. syst. error: $\lesssim 10\%$

$SU(3)$: $T_c \simeq 284 \pm 10\,\text{MeV}$ $\qquad T_c/\sqrt{\sigma} = 0.646 \pm 0.023$

num. accuracy $\qquad$ lattice: 0.646

(bed-up)

(1) • $\kappa_A = -2\,\kappa_c$: $\boxed{\kappa_c > \frac{d-3}{4}}$

$d=4$: $\kappa_c > 1/4$

• FRG/DSE : $\kappa_c = 0.593$:

• lattice : $\kappa_A \sim -1$, $\kappa_c \sim 0$

$$(4-2) + (4-1)\overset{\kappa_A}{(-1)} - 2\cdot 0 \simeq -1 < 0$$

Numerics:

SU(2) : $T_c \simeq 276 \pm 10\,\mathrm{MeV}$ $\quad T_c/\sqrt{\sigma} = 0.614 \pm 0.02$

lattice : $T_c/\sqrt{\sigma} = 0.709$

SU(3) : $T_c \simeq 284 \pm 10\,\mathrm{MeV}$ $\quad T_c/\sqrt{\sigma} = 0.646 \pm 0.02$

lattice : $T_c/\sqrt{\sigma} = 0.646$

Final Remarks:

(1) T-dep. of props

back reaction of $V[A_0]$; in part. for SU(2)

(2) Fermions : • chiral phase boundary $N_f = 2$

• hadronisation

• finite μ